Abstract

This work presents a physics-infused reduced-order modeling (PIROM) framework towards the design, analysis, and optimization of ablating hypersonic thermal protection systems (TPS).

1 Introduction

At hypersonic speeds, aerospace vehicles experience extreme aero-thermal environments that requires specialized thermal protection systems (TPS) to shield internal sub-structures, electronics, and possibly crew members from the intense aerodynamic heating. The TPS is often composed of ablating materials – a high-temperature capable fibrous material injected with a resin that fills the pore network and strengthens the composite Amar2016. The TPS design promotes the exchange of mass through thermal and chemical reactions (i.e., pyrolisis), effectively mitigating heat transfer to the sub-structures.

As a result, accurate prediction for the ablating TPS response under extreme hypersonic heating becomes fundamental to ensuring survivability, performance, and safety of hypersonic vehicles. Not only is it necessary to assess the performance of the thermal management systems, but also the shape changes of the vehicle's outer surface induced by the ablating material, and its impact on the aerodynamics, structural integrity, and controllability. Unfortunately, high-fidelity simulations of ablating TPS remains a formidable challenge both theoretically and computationally.

On the theoretical side, the thermo-chemical reactions, coupled with the irregular pore network structure, translate into simplifying assumptions to reduce non-linearities, and make the resulting equations more amenable for engineering application and design analysis x. For instance, one of the most notable codes is the one-dimensional CMA code that was developed by Aerotherm Corporation in the 1960s Howard2015. Despite its practical use in...

Another example is the CHarring Ablator Response (CHAR) ablation code, which ignores elemental decompositions of the pyrolizing gases, assumes the gases to be a mixture of perfect gases in thermal equilibrium, and assumes no reaction or condensation with the porous network [**?**].

theoretically:

computationally:

2 Modeling of Ablating Thermal Protection Systems

This section presents the ablation problem for a non-decomposing TPS as a parametrized system of non-linear PDEs. These non-linear PDEs govern the energy of heat conduction and the pseudo-elastic material deformation of the mesh motion. Two different but mathematically-connected numerical solution strategies are provided: (1) a high-fidelity full-order model (FOM) based on a discontinuous Galerkin FEM, and (2) a thermo-elastic RPM based on a one-dimensional approximation to the energy and pseudo-elasticity equations.

2.1 Governing Equations

Consider a generic domain $\Omega \subset$, $d = 2$ or 3, illustrated in Fig. 1. A heat flux $q_b(x,t)$ is prescribed on the boundary Γ_q (i.e., Neumann boundary condition), and the temperature $T_b(x,t)$ is prescribed on boundary Γ_T (i.e., Dirichlet boundary condition), where $\Gamma_q \cup \Gamma_T = \partial\Omega$ and $\Gamma_q \cap \Gamma_T = \emptyset$. The ablation occurs only on the heated boundary Γ_q, and its effects are included into the energy equation using an Arbitrary Lagrangian-Eulerian (ALE) description. The ALE assumes that the displacement $\mathbf{w}(x,t) \in \mathbb{R}^d$ of the computational mesh moves with velocity $\mathbf{v}(x,t)$ that is different to the material velocity, which is fixed to zero in this work.

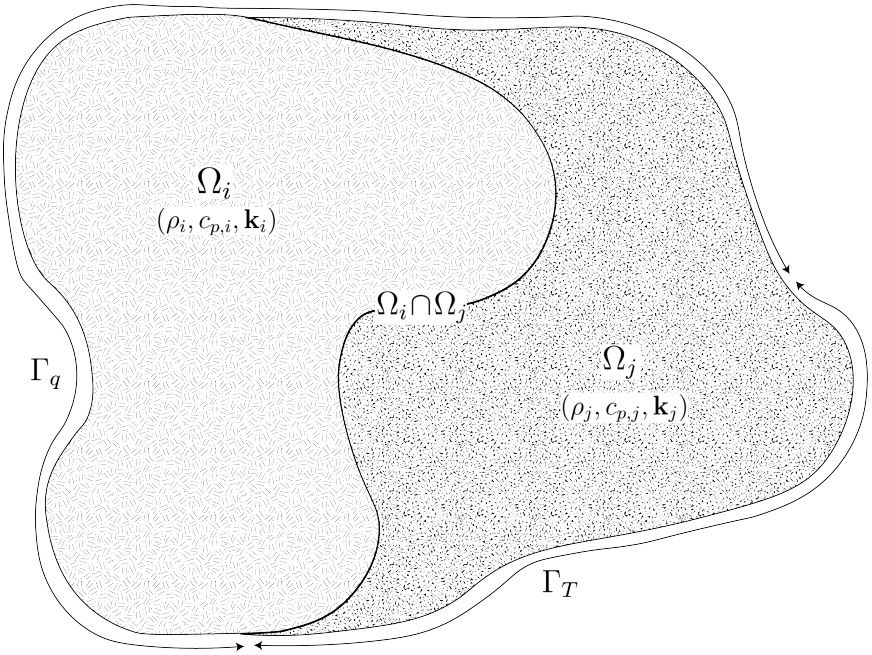

Figure 1: General domain Ω with prescribed heat flux $q_b(x,t)$ and temperature $T_b(x,t)$ on the boundaries Γ_q and Γ_T, respectively. The mesh moves with a velocity $\mathbf{v}(x,t)$, while the material velocity is $\mathbf{w}(x,t)$. draw mesh next to arbitrary domain with moving boundaries.

The transient heat conduction is described by the energy equation,

$$\rho c_p \left(\frac{\partial T}{\partial t} - \mathbf{v}(x,t) \cdot \nabla T \right) - \nabla \cdot (\mathbf{k} \nabla T) = \mathcal{Q}(x,t), \ x \in \Omega \tag{1a}$$

$$-\mathbf{k}\nabla T \cdot \mathbf{n} = q_b(x,t), \ x \in \Gamma_q \tag{1b}$$

$$T(x,t) = T_b(x,t), \ x \in \Gamma_T \tag{1c}$$

$$T(x,0) = T_0(x), \ x \in \Omega \tag{1d}$$

while the mesh motion is described by the pseudo-elasticity equation,

$$\nabla \cdot \boldsymbol{\sigma}(\mathbf{w}) = 0 \tag{2a}$$

$$\mathbf{w}(x,t) = \mathbf{w}_q(x,t), \quad x \in \Gamma_q \tag{2b}$$

$$\mathbf{w}(x,t) = 0, \quad x \notin \Gamma_q \tag{2c}$$

$$\mathbf{w}(x,0) = \mathbf{0} \tag{2d}$$

The density ρ, heat capacity c_p, and thermal conductivity $\mathbf{k} \in \mathbb{R}^{n_d \times n_d}$ are assumed to be constant with respect to temperature in this work. The terms in eq. (1a), in the order they appear, correspond to the unsteady energy storage, heat conduction, temperature advection due to mesh motion, and the heat source terms.

The elasticity equation eq. (2a) states that the divergence of the stress tensor $\boldsymbol{\sigma}(\mathbf{w})$ is zero. The stress tensor is related to the strain tensor $\boldsymbol{\epsilon}(\mathbf{w})$ through Hooke's law,

$$\boldsymbol{\sigma}(\mathbf{w}) = \mathbb{D} : \boldsymbol{\epsilon}(\mathbf{w})$$

where $\mathbb{D}$ is the constitutive operator, ":" is the double contraction of tensors, and $\boldsymbol{\epsilon}$ is the symmetric strain tensor given by,

$$\boldsymbol{\epsilon}(\mathbf{w}) = \frac{1}{2} \left(\nabla \mathbf{w} + \nabla \mathbf{w}^T \right)$$

For instance, an isotropic material assumption results in,

$$\boldsymbol{\sigma} = \lambda \left(\nabla \cdot \mathbf{w}\right) \mathbf{I} + 2\mu \boldsymbol{\epsilon}(\mathbf{w})$$

where λ and μ are Lame constants that are arbitrarily selected to model the mesh motion. The "material" properties λ and μ can be chosen to tailor the mesh deformation and need not represent the actual material being modeled Amar2016.

The boundary conditions for the energy equation includes a heated surface (eq. (1b)) and a constant-temperature surface (eq. (1c)). The boundary conditions for the pseudo-elasticity equation are a function of the surface temperature $T_q(x,t)$ for $x \in \Gamma_q$ using a B' table. The B' table....

$$\mathbf{w}_q(x,t) = \int_0^t \mathbf{v}(x,\tau) d\tau = \int_0^t \mathbf{f}\left(T_q(x,\tau)\right) d\tau \tag{3}$$

2.2 Full-Order Model: Finite-Element Method

To obtain the full-order numerical solution, the governing equation is spatially discretized using variational principle of Discontinuous Galerkin (DG) to result in a high-dimensional system of ODEs for the time-varying nodal data. The full-order TPS ablation simulations are computed using standard FEM instead, and the equivalence between DG and standard FEM is noted upon their convergence.

Consider a conforming mesh partition domain, where each element belongs to one and only one component. Denote the collection of all M elements as $\{E_i\}_{i=1}^M$. In an element E_i, its shared boundaries with another element E_j, Neumann BC, and Dirichlet BC are denoted as e_{ij}, e_{iq}, and e_{iT}, respectively. Lastly, $|e|$ denotes the length ($n_d = 2$) or area ($n_d = 3$) of a component boundary e.

For the i-th element, use a set of $n^{(i)}$ trial functions, such as polynomials, to represent the temperature distribution,

$$T^{(i)}(x,t) = \sum_{i=1}^{n^{(i)}} \phi_i^{(i)}(x) u_i^{(i)} \equiv \boldsymbol{\phi}^{(i)}(x)^T \mathbf{u}^{(i)}(t) \tag{4}$$

Without loss of generality, the trial functions are assumed to be orthogonal, so that $\int_{E^{(i)}} \phi_k^{(i)}(x)\phi_l^{(i)}(x)dx = \left|E^{(i)}\right| \delta_{kl}$, where $\left|E^{(i)}\right|$ is the area ($n_d = 2$) or volume ($n_d = 3$) of the i-th element, and δ_{kl} is the Kronecker delta. Furthermore, for simplicity, choose $\phi_1^{(i)}(x) = 1$; by orthogonality $\int_{E^{(i)}} \phi_l^{(i)}(x)dx = 0$ for $l \neq 1$. Under this choice of basis, $u_1^{(i)}$ represents the average temperature in the i-th element.

By standard variational processes, e.g., Cohen2018, the full governing equation is denoted as,

$$\mathbf{A}(\mathbf{u})\dot{\mathbf{u}} = \left[\mathbf{B}(\mathbf{u}) + \mathbf{C}(t)\right] \mathbf{u} + \mathbf{f}(t) \tag{5}$$

where $\mathbf{u} = \left(\mathbf{u}^{(1)}, \mathbf{u}^{(2)}, \ldots, \mathbf{u}^{(M)}\right)^T \in \mathbb{R}^{n_d M}$ includes all the DG variables, $\mathbf{f} \in \mathbb{R}^{n_d M}$ is the external forcing, and the system matrices $\mathbf{A}$, $\mathbf{B}$, and $\mathbf{C}$ are due to heat capacity, heat conduction, and mesh advection, respectively. The detailed formulation of the DG model is provided in Appendix DG-FEM.

2.3 Reduced-Physics Model: One-Dimensional Thermo-Elastic Solver

In this section, the main results regarding the derivation of the thermo-elastic RPM are presented, and the details are provided in Appendix x. The RPM models one-dimensional temperature distribution and mesh displacements for an ablating TPS over a series of interconnected components. Over each element, the governing dynamics are simplified using a coarse-grained FEM approach, with the mesh motion predicted based on an analytical solution to the elasticity equations.

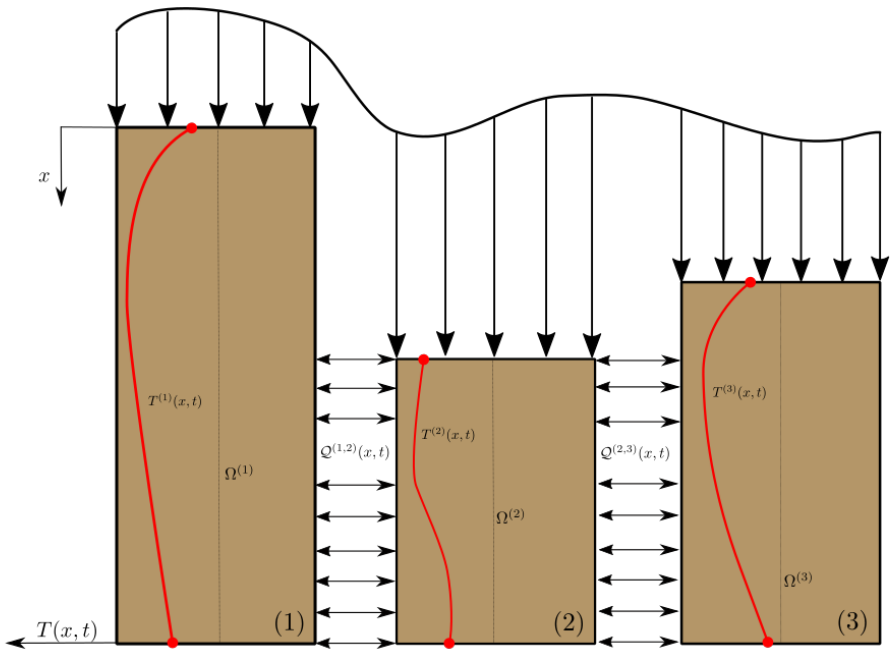

Figure 2: Partition of the TPS into three one-dimensional components.

2.3.1 Finite-Element Method and Component Interactions

The arbitrary domain in Fig. 1 is partitioned into N components $\{\Omega^{(i)}\}_{i=1}^{N}$, each with $\left\{E_j^{(i)}\right\}_{j=1}^{n^{(i)}}$ finite elements, establishing the resolution for the temperature and mesh displacement fields over each component. Figure x shows a partition of the TPS into $N = M = 3$, where the top and bottom are subject to Neumann and adiabatic boundary conditions, respectively.

A first-order FEM scheme is adopted for each component, which results in a block-diagonal system of ODEs for the nodal temperature values of the components,

$$\mathbf{A}\left(\bar{\mathbf{u}}\right)\dot{\bar{\mathbf{u}}} = \left(\mathbf{B} + \mathbf{C}(t)\right)\bar{\mathbf{u}} + \mathbf{f}\left(\bar{\mathbf{u}}, t\right) \tag{6}$$

where the block matrices are defined as,

$$\begin{aligned}
\mathbf{A}_{ij} &= \begin{cases} \mathbf{A}^{(i)}(\bar{\mathbf{u}}^{(i)}), & i = j \\ 0, & i \neq j \end{cases} \qquad \mathbf{C}_{ij}(t) = \begin{cases} \mathbf{C}^{(i)}(t), & i = j \\ 0, & i \neq j \end{cases} \\
\mathbf{B}_{ij} &= \begin{cases} \mathbf{B}^{(i)}(\bar{\mathbf{u}}^{(i)}), & i = j \\ 0, & i \neq j \end{cases} \qquad \mathbf{f}_i(\bar{\mathbf{u}}, t) = \begin{cases} \mathbf{f}_{\mathrm{BC}}^{(i)}(t) + \mathbf{f}_{\mathcal{Q}}^{(i)}(\bar{\mathbf{u}}, t), & i = j \\ \mathbf{0}, & i \neq j \end{cases}
\end{aligned} \tag{7a}$$

where $\mathbf{f}_{\mathrm{BC}}$ and $\mathbf{f}_{\mathcal{Q}}$ are the boundary and component-level energy sources.

The energy sources are modeled using distributed volumetric energies $\left\{\mathcal{Q}_{\mathrm{net}}^{(i)}(x,t)\right\}_{i=1}^{N}$, where the net energy source into the i-th component is defined as,

$$\mathcal{Q}_{\mathrm{net}}^{(i)}(x,t) = \sum_{j \in \mathcal{N}_i} Q^{(i,j)}(x,t) \tag{8}$$

and the heat transfer between components i and j is approximated as,

$$Q^{(i,j)}(x,t) = \frac{T^{(j)}(x,t) - T^{(i)}(x,t)}{R_{(i,j)}} \tag{9}$$

Thus, the $\mathbf{f}_{\mathcal{Q}}$ term in eq. (7a) becomes,

$$\mathbf{f}_{\mathcal{Q}}^{(i)}(\bar{\mathbf{u}}, t) = \sum_{j \in \mathcal{N}_i} \frac{1}{R_{(i,j)}} \left(\mathbf{M}^{(i,j)} \bar{\mathbf{u}}^{(j)}(t) - \mathbf{M}^{(i,i)} \bar{\mathbf{u}}^{(i)}(t) \right) \tag{10}$$

where $\mathbf{M}^{(i,j)}$ and $\mathbf{M}^{(i,i)}$ are due to

2.3.2 Coarse Graining

Consider a DG model as in eq. (5) for M components and N elements; clearly $N \gg N$. Let $\mathcal{V}_j = \left\{ i | E^{(i)} \in \Omega^{(j)} \right\}$ be the indices of the elements belonging to the j-th component, so $E^{(i)} \in \Omega^{(j)}$ for $i \in \mathcal{V}_j$; number of elements in $\Omega^{(j)}$ is denoted as $|\mathcal{V}_j|$.

The ablation on the i-th component is modeled using a one-dimensional approximation to the temperature and mesh-motion equations in eq. (1d), and are given by,

$$\rho c_p \left(\frac{\partial T^{(i)}}{\partial t} - v^{(i)}(x,t) \frac{\partial T^{(i)}}{\partial x} \right) - \frac{\partial}{\partial x} \left(k \frac{\partial T^{(i)}}{\partial x} \right) - \mathcal{Q}_{\text{net}}^{(i)}(x,t) = 0 \tag{11a}$$

$$\frac{\partial}{\partial x} \left(\frac{\partial u^{(i)}}{\partial x} \right) = 0 \tag{11b}$$

with boundary conditions for the energy equation,

$$-k \frac{\partial T^{(i)}}{\partial x} \bigg|_{x=0} = q_b^{(i)}(t) \tag{12a}$$

$$-k \frac{\partial T^{(i)}}{\partial x} \bigg|_{x=\ell} = 0 \tag{12b}$$

and for the elasticity equation,

$$u^{(i)}(0,t) = \int_{t_0}^{t} v^{(i)}(\tau) d\tau = \int_{0}^{t} f(T_w^{(i)}(\tau)) d\tau \tag{13a}$$

$$u^{(i)}(\ell, t) = 0 \tag{13b}$$

where $v^{(i)}(t)$ is the surface receding velocity due to ablation, which is a function of the surface temperature as in eq. (3). The surface velocity is computed from a cubic spline interpolate to a B' look-up table...

2.3.3 Thermal Solver

The FEM implementation details are supplied in Appendix x. For the n-th component, the result of the FEM discretization is a system of ODEs for the nodal temperatures, coupled to the neighboring component $n+1$ through the energy volumetric source term,

$$\mathbf{A}^{(i)} \frac{d\mathbf{T}^{(i)}}{dt} + \left(\mathbf{B}^{(i)} - \mathbf{C}^{(i)}(t) \right) \mathbf{T}^{(i)} = \mathbf{f}^{(i)}(t) \tag{14}$$

where,

- $\mathbf{A}^{(i)} \in \mathbb{R}^{M \times M}$ is the mass matrix,
- $\mathbf{B}^{(i)} \in \mathbb{R}^{M \times M}$ is the stiffness matrix,
- $\mathbf{C}^{(i)}(t) \in \mathbb{R}^{M \times M}$ is the advection matrix,,

- $\mathbf{T}^{(i)} \in \mathbb{R}^M$ is the vector of nodal temperatures, and
- $\mathbf{f}^{(i)}(t) \in \mathbb{R}^M$ is the input vector, which includes the Neumann boundary conditions and the net volumetric energy source term $\mathcal{Q}^{(i)}_{\text{net}}$.

where M is the number of nodes in the one-dimensional mesh for the i-th component.

2.3.4 Pseudo-Elastic Solver

Note that eq. (11b) is steady. Under the assumption that the mesh deformation is quasi-steady, it can be applied at each time step within an ablation simulation. For instance, a known value of the wall temperature $T_w(t)$ specifies a Dirichlet boundary condition for the displacement, and the resulting nodal displacements within the ablator are determined from eq. (2a).

Along the one-dimensional domain, the PDE in eq. (2a) simplifies to,

$$\frac{\partial^2 u^{(i)}}{\partial x^2} = 0 \tag{15}$$

which has the analytical solution,

$$u^{(i)}(x,t) = a(t)x + b(t) \tag{16}$$

Imposing the boundary conditions leads to,

$$u^{(i)}(x,t) = u^{(i)}(0,t)\left(\frac{x_1^{(i)} - x}{h^{(i)}}\right) \tag{17}$$

The mesh velocity is the time derivative of the displacement,

$$v^{(i)}(x,t) = \frac{\partial u^{(i)}(x,t)}{\partial t} = v^{(i)}(t)\left(\frac{x_1^{(i)} - x}{h^{(i)}}\right) \tag{18}$$

2.3.5 Coupling Scheme

2.3.6 Reduced-Physics Ablation Simulation

A Numerical Implementation

A.1 Full-Order Model

A.2 Reduced-Physics Model

This section outlines the FEM implementation for the $N = 3$ one-dimensional interconnected components used in Sec. x. Consider over the i-th element in Fig. x the linear basis,

$$\phi_1^{(i)}(x) = 1, \quad \phi_2^{(i)}(x) = \frac{2}{h^{(i)}}\left(x - x_c^{(i)}\right), \quad x \in \Omega^{(i)} = \left[x_0^{(i)}, x_1^{(i)}\right]$$

where $h^{(i)} = x_1^{(i)} - x_0^{(i)}$ and $x_c^{(i)} = (x_0^{(i)} + x_1^{(i)})/2$. The

The weak form of the

Multiply through by the weight function $\phi_j(x)$ and integrate over the domain $\Omega^{(i)}$,

$$\int_{\Omega^{(i)}} \left[\rho c_p\left(\frac{\partial T^{(i)}}{\partial t} - v^{(i)}(x,t)\frac{\partial T^{(i)}}{\partial x}\right) - \frac{\partial}{\partial x}\left(k\frac{\partial T^{(i)}}{\partial x}\right) - \mathcal{Q}^{(i)}_{\text{net}}(x,t)\right]\phi_l^{(i)}(x)dx = 0 \tag{19}$$

Using integration by parts the natural boundary conditions are obtained,

$$\int_{\Omega^{(i)}} \rho c_p \phi_l^{(i)}(x) \frac{\partial T^{(i)}}{\partial t} dx = -\int_{\Omega^{(i)}} k \frac{\partial T^{(i)}}{\partial x} \frac{\partial \phi_l^{(i)}(x)}{\partial x} dx + \int_{\Omega^{(i)}} \rho c_p v(x,t) \phi_l^{(i)}(x) \frac{\partial T^{(i)}}{\partial x} dx + k \frac{\partial T^{(i)}}{\partial x} \phi_l^{(i)}(x) \Big|_{\partial\Omega} + \int_{\Omega^{(i)}} \phi_l^{(i)}(x) \mathcal{Q}_{\text{net}}^{(i)}(x,t) dx \tag{20}$$

Perform the finite-element approximation,

$$T^{(i)}(x,t) \approx \sum_{k=1}^{n^{(i)}} \bar{u}_k^{(i)}(t) \phi_k^{(i)}(x) \tag{21}$$

and define the matrix elements,

$$A_{kl}^{(i)} = \int_{\Omega^{(i)}} \rho c_p \phi_k^{(i)}(x) \phi_l^{(i)}(x) dx \tag{22}$$

$$B_{kl}^{(i)} = -\int_{\Omega^{(i)}} k \frac{\partial \phi_k^{(i)}(x)}{\partial x} \frac{\partial \phi_l^{(i)}(x)}{\partial x} dx \tag{23}$$

$$C_{kl}^{(i)}(t) = \int_{\Omega^{(i)}} \rho c_p v^{(i)}(x,t) \phi_l^{(i)}(x) \frac{\partial \phi_k^{(i)}}{\partial x} dx \tag{24}$$

$$f_l^{(i)}(t) = k \frac{\partial T}{\partial x} \phi_l^{(i)}(x) \Big|_{\partial\Omega} + \int_{\Omega^{(i)}} \phi_l^{(i)}(x) \mathcal{Q}_{\text{net}}^{(i)}(x,t) dx \tag{25}$$

The semi-discrete form of the energy equation for the nodal temperatures $\bar{\mathbf{u}} \in \widetilde{\approx}$, including the ALE-induced advection effects from mesh motion, is given as,

$$\mathbf{A}\dot{\bar{\mathbf{u}}} = (\mathbf{B} + \mathbf{C}(t))\, \bar{\mathbf{u}} + \bar{\mathbf{f}}(t) \tag{26}$$

The thermodynamic interaction between the components is modeled via the net volumetric energy source from eq. (8), which for the three-components in Fig. x are described by,

$$\mathcal{Q}_{\text{net}}^{(1)}(x,t) = -\mathcal{Q}^{(1,2)}(x,t) \tag{27a}$$

$$\mathcal{Q}_{\text{net}}^{(2)}(x,t) = \mathcal{Q}^{(1,2)}(x,t) - \mathcal{Q}^{(2,3)}(x,t) \tag{27b}$$

$$\mathcal{Q}_{\text{net}}^{(3)}(x,t) = \mathcal{Q}^{(2,3)}(x,t) \tag{27c}$$